A Novel Electromechanical Actuation Mechanism of a Carbon Nanotube Fiber

*Wenhan Guo, Chao Liu, Fangyuan Zhao, Xuemei Sun, Zhibin Yang, Tao Chen, Xuli Chen, Longbin Qiu, Xinhua Hu, and Huisheng Peng**

Carbon nanotubes (CNTs) have been extensively studied as a functional material for over two decades due to their unique structures and remarkable properties.[1–11] It has been well demonstrated that CNTs are light-weight and have an extremely high surface area, e.g., ~1600 m^2 g^{-1} for single-walled CNTs, they are the strongest material ever discovered by human kind, and they exhibit a high electrical conductivity of 10^5 S cm^{-1}.[11] To further improve their practical applications, it is necessary to assemble CNTs into macroscopically continuous fibers in which CNTs are highly aligned to retain the excellent properties of individual CNTs.[6–11] For instance, CNT fibers were found to be much stronger and stiffer than various engineering fibers, and were proposed as a family of high-performance structural materials.[9] In addition, due to a high conductivity on the level of 10^3 S cm^{-1}, they were also used as electrodes to fabricate high-efficiency dye-sensitized solar cells or incorporated into conjugated polymers such as chromatic polydiacetylene to produce a unique color change in response to current.[10,11]

Recently, Spinks and co-workers have pioneered another new and important application direction by using CNT fibers as promising electromechanical actuators with the conversion of electrical energy into mechanical energy.[5] Compared with other actuation materials such as ferroelectric and electrostrictive materials, conducting polymers, and polymer gels,[12–17] the CNT fiber exhibited a unique torsional rotation by a three-electrode electrochemical system in an electrolyte. A hydrostatic actuation mechanism explained the electromechanical torsion.

Herein, we further discover that the electromechanical torsion of CNT fibers occurs in almost all available environmental media such as air, water, and organic solvents in addition to electrolytes. In addition, the torsion of our CNT fibers can be produced by directly passing the current along them, without the use of a relatively complex three-electrode electromechanical setup.[5] A different mechanism, Ampere's Law among helically aligned CNTs, explains the simultaneous occurrence of lengthwise contraction and rotary torsion upon applying a low current. Table S1, Supporting Information, compares our CNT fibers with other widely studied actuation materials. The CNT fiber can produce a stress over 100 times that of the strongest natural skeletal muscle with high reversibility, good stability, high work density, extremely low functioning electric field, and application to various media. The combined excellent properties provide the CNT fiber actuator with promising applications in many fields. In this work, as a way of example, the use of torsional fibers for electric motors is demonstrated. In addition, the mechanism based on Ampere's Law at the nanometer scale can be also generalized to develop a series of electromechanically torsional materials through the helical and aligned arrangement of conductive one-dimensional nanostructures such as nanorods and other nanotubes.

Spinnable CNT arrays were first synthesized by a chemical vapor deposition process, and the CNTs typically had a multi-walled structure with a diameter of ~10 nm. CNT fibers were then spin-drawn from the array (Movie S1, Supporting Information). **Figure 1** shows scanning electron microscopy (SEM) images of the spun CNT fibers which had diameters of 16–20 μm. Both right-handed (Figure 1a) and left-handed (Figure 1b) rotations were obtained by simply changing the spinning direction. Figure 1c further indicates that CNTs are highly aligned in the fiber. The helical angle of the CNT fiber defined in Figure 1a could be tuned by varying the spinning rate at a fixed drawing speed of 2 mm s^{-1}. As expected, the helical angle was generally increased with the increase in spinning rate. For instance, a spinning rate of 1300 rounds per minute produced a helical angle of ~25°, while a higher rate of 2700 rounds per minute increased the helical angle to ~51°. Because the CNT fibers in this work were spin-drawn from the same CNT array by using the same width of CNT ribbon at the starting point, the as-prepared fiber had a similar CNT number density of ~5.5×10^{11} cm^{-2}. In order to further improve their uniformity and properties, the as-prepared CNT fibers were post-treated in ethanol. The diameters of the resulting CNT fibers were decreased by ~1 μm on average, and their tensile strengths increased to 800 MPa.

The actuation of the spun CNT fiber was first investigated in air. **Figure 2**a schematically shows the electromechanical response of a left-handed CNT fiber. When subjected to a direct current of several microamperes, the fiber shrank along the axial direction, and the two ends rotated in opposite directions that increased the helical angle at the same time. The

W. Guo, C. Liu, X. Sun, Z. Yang, T. Chen, X. Chen, L. Qiu, Prof. H. Peng
State Key Laboratory of Molecular Engineering of Polymers
Department of Macromolecular Science and Laboratory of Advanced Materials
Fudan University
Shanghai 200438, P. R. China
E-mail: penghs@fudan.edu.cn
F. Zhao, Prof. X. Hu
Department of Materials Science and Key Laboratory of Micro and Nano Photonic Structures (Ministry of Education)
Fudan University
Shanghai 200438, P. R. China.

DOI: 10.1002/adma.201201845

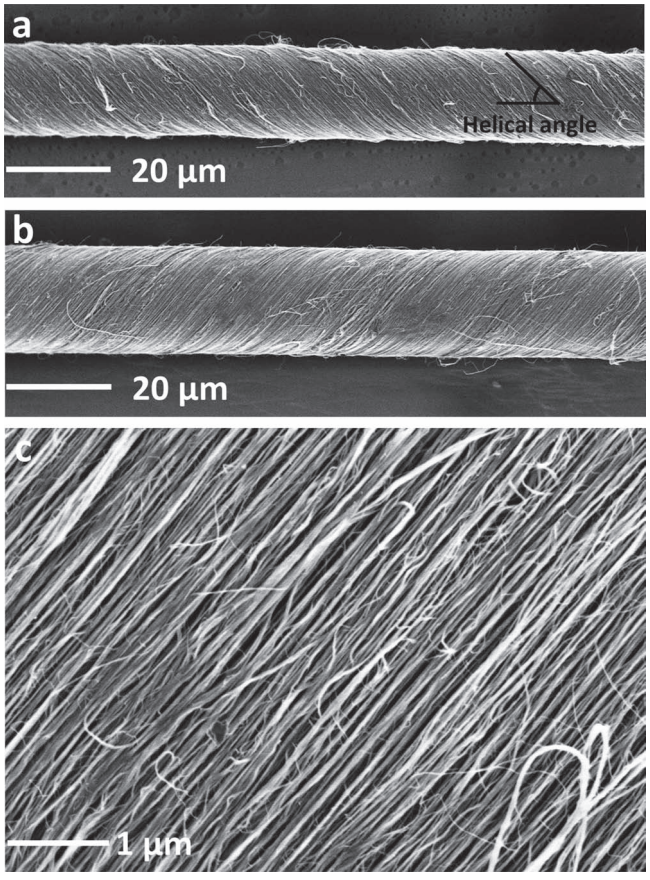

Figure 1. SEM images of CNT fibers. a) A CNT fiber with right-handed rotation. b) A CNT fiber with left-handed rotation. c) Higher magnification of (b). Helical angle is defined and shown in (a).

contractive strain and rotary angle were typically higher than 2% and larger than 360°, respectively. Upon removal of the current, the CNT fiber fully rotated back to the original state. A typical contraction process of a CNT fiber with a length of 5 mm is presented in Movie S2, Supporting Information. The two ends of the fiber were fixed by silver paste and connected to an external current source. The CNT fiber was slightly bent to create a three dimensional geometry at the original state, and subjected to a pulsed current between 0 and 4 mA with a frequency of 1 Hz. The fiber shrank in length and became tightened upon the passage of current, and then recovered to the original bent state once the current was removed. This contractive response could be repeated for over two thousand cycles without decay. The torsional rotations of left-handed CNT fibers are presented in Movies S3 and S4, and the experimental setup of Movie S4 is shown in Figure S2, Supporting Information. In the case of right-handed CNT fibers, the same lengthwise contraction and rotary torsion were also observed. For any CNT fiber, the direction change of the currents with the same value did not affect the rotary direction or the speed, while increasing the current level enhanced the rotation degree, which is confirmed in Movie S5, Supporting Information. The right part of a right-handed CNT fiber continuously rotated along an anti-clockwise direction with the increase in current from 0 to 5 mA, and then reversibly rotated back (in a clockwise direction) step by step with the gradual decrease of the current from 5 to 0 mA. The above experiments were performed in air. We also investigated other environmental media of various liquids such as water, organic solvents, and electrolyte solutions, and the same phenomena of lengthwise contraction and rotary torsion were observed for spun CNT fibers. A series of videos which appear the same as Movies S2, S3, and S5 have been recorded in liquid (not provided for clarity), and the actuation speed seemed close to that in air. To simplify the discussion, left-handed CNT fibers will be mainly described in air unless stated otherwise. A current range up to 5 mA was mainly studied according to the general application requirement, and the corresponding electric field was up to 1 kV m^{-1}. It should be noted that the actuation mainly depended on the current density for the same CNT fiber. Therefore, CNT fibers with larger diameters require higher currents to be actuated, while the produced stress remained almost unchanged.

The CNT fiber exhibited good electromechanical reversibility. Figure 2b shows the produced stresses of a 5 mm long CNT fiber after being passed with a pulsed current between 0 and 4 mA for over 1200 s. As it took 6 s for a pulse period, more than 200 cycles had been made for the CNT fiber. Figure 2c summarizes the relationship between produced stress and cycle number based on the data in Figure 2b. No obvious decrease in the produced stress was found with pulsed currents. In addition, no structural changes had been traced by SEM. Furthermore, the CNT fiber underwent a stable response of producing stress after pass with repeated current pulses for over 4 h without any discernible decay in the actuation capability under atmospheric conditions. In other words, the CNT fiber shows a reversible torsional actuation after 2400 cycles, which is critical for actuator materials.[15–17]

Both lengthwise contraction and torsional rotation of the CNT fiber were fast (< 0.4 s), so the actuation responses could be further traced in situ by use of linearly increasing and then decreasing currents. The bottom graph in Figure 2d shows the currents used which first increased linearly from 0 to 5 mA in 25 s and then decreased linearly from 5 to 0 mA in another 25 s for a CNT fiber with length of 5 mm. The fiber did not produce an obvious stress at a current lower than ~2 mA but showed a significant increase beyond this current point (the top graph in Figure 2d). Based on the fitting curve in Figure 2d, the relationship between produced stress (F) and current (I) can be approximately expressed as $F \propto I^2$.

The CNTs in the spun fiber function similarly to conductive wires when a current is applied. According to Ampere's Law, these CNTs in a parallel arrangement produce electromagnetic forces as the current flows along the length of the CNTs. Although the electromagnetic force of a single CNT is very small, the collective effect of more than a million CNTs in the cross-sectional area of a fiber can generate a force high enough to induce macroscopic electromechanical actuation of lengthwise contraction and torsional rotation. In the case of contraction, the electromagnetic attractions are perpendicular to the CNTs, and the contraction stress corresponds to the component force along the axial direction of the CNT fiber. Therefore, for CNT fibers with the same cross-sectional

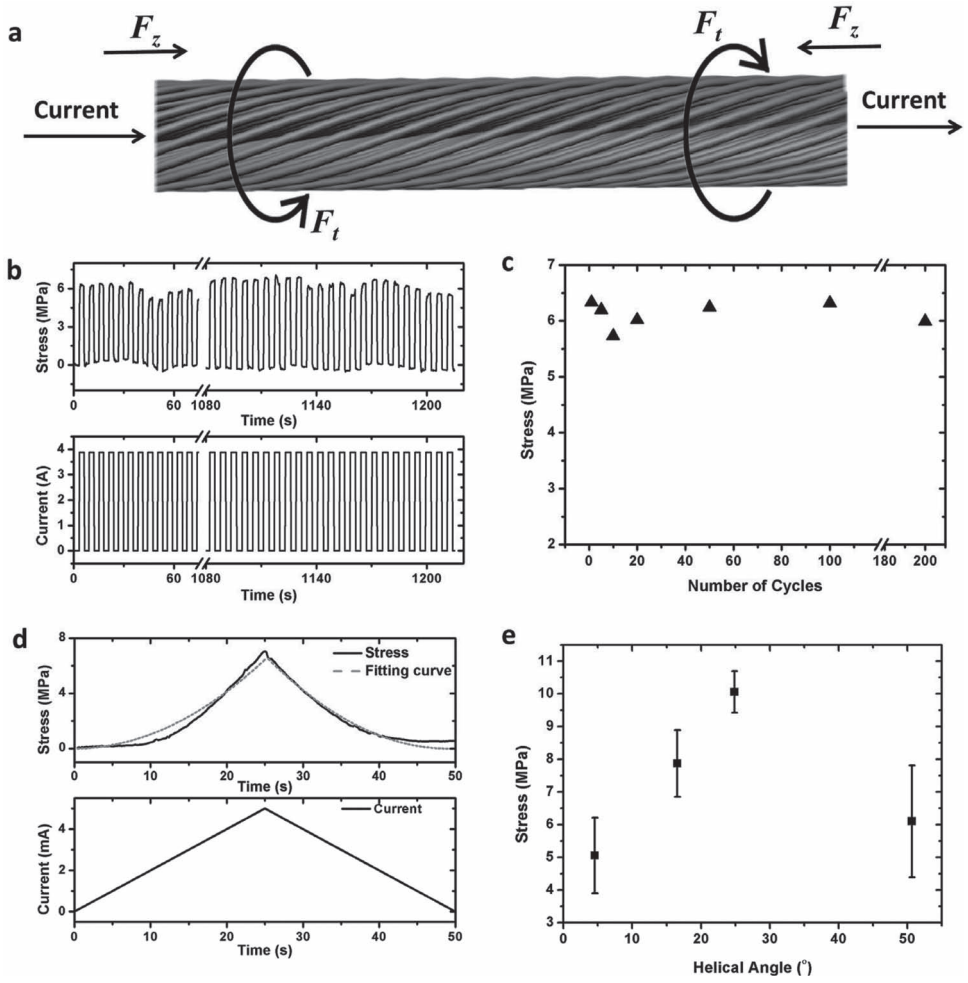

Figure 2. Lengthwise contraction and rotary torsion of a CNT fiber. a) Schematic illustration of the lengthwise contraction and rotary torsion of a CNT fiber upon the passage of current. F_z and F_t represent the contractive and torsional forces, respectively. b) The stress produced by a CNT fiber upon passing a pulsed current. c) Dependence of the produced stress on the pulsed current cycle number obtained at (b) .d) In situ monitoring of the produced stress when the used current was linearly increased and then decreased. e) Dependence of the stress on helical angle in a CNT fiber with the same current of 5 mA. The data of this figure were obtained from CNT fibers with the same length of 5 mm.

CNT number density but different helical angles, the produced stress should increase with the increasing helical angle. In addition, the distance among CNTs in their perpendicular direction decreases with increasing helical angle, which should also increase the produced stress. Unexpectedly, for a CNT fiber with a length of 5 mm, the stress first increased and then decreased with the increasing helical angle (Figure 2e). The peak value of the produced stress appeared at a helical angle between 25° and 50°. This unusual phenomenon may be ascribed to the three-dimensional hopping conduction mechanism of the CNT fiber.[6–9] We have previously found that the relationship between electrical conductivity and temperature in a CNT fiber follows Mott's hopping model which can be expressed as $\sigma \propto \exp(-A/T^{[1/(d+1)]})$, where A is a constant and d is the dimensionality.[8,9] By fitting $\ln\sigma$ and T under different dimensions of one, two, and three, it was concluded that the electron transport is consistent with a three-dimensional hopping mechanism (Figure S3, Supporting Information). Therefore, electrons may hop among neighboring CNTs besides being transported along their length when a current passes through the fiber. In other words, the fiber resistance is composed of two parts, i.e., the contact resistances among CNTs and the resistances of the individual CNTs. With the increase of helical angle in the fiber, the distance among CNTs decreases, which reduces the contact resistances, while the resistances of the individual CNTs remains almost unchanged. Therefore, more and more electrons hop among CNTs rather than transport along the axis, and this hopping conduction does not contribute to the attraction among CNTs which will be provided in the following discussion. The electromagnetic interaction in the fiber decreases with the increasing helical angle for the same value of the applied current. The above opposite factors lead to the appearance of a critical helical

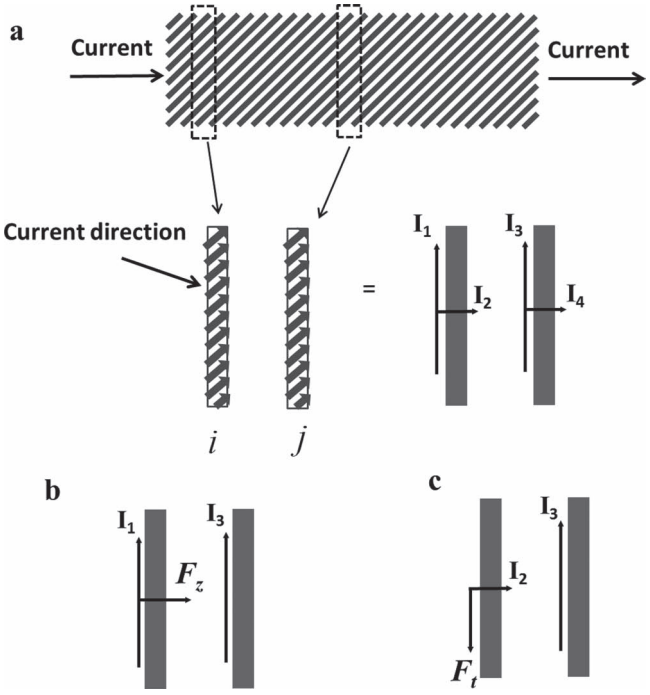

Figure 3. Mechanism for the lengthwise contraction and rotary torsion. a) Schematic illustration of two parallel disks of *i* and *j* in the CNT fiber. The lines in the fiber correspond to individual CNTs. b,c) Schematic illustration of the interactions between the two disks. The electric currents of the left and right disk are decomposed into I_1 and I_2 and I_3 and I_4, respectively.

angle. The highest stress produced by a CNT fiber was over 10 MPa, more than 100 times that of the strongest natural skeletal muscle.[17]

Ampere's Law among helically aligned CNTs explains the simultaneous occurrence of lengthwise contraction and rotary torsion upon applying a low current. A CNT fiber can be considered as many parallel disks with the same thickness along the fiber (**Figure 3**a). For any two disks (labeled as disk *i* at left and disk *j* at right), the electric currents at left and right can be decomposed into I_1 and I_2 and I_3 and I_4, respectively (Figure 3a). I_1 and I_3 are perpendicular to the axial direction, while I_2 and I_4 go along the axial direction of the CNT fiber. According to Ampere's Law, I_3 exerts an attractive electromagnetic force (F_z) on I_1 (Figure 3b), while I_3 exerts a torsional electromagnetic force (F_t) on I_2 (Figure 3c). Therefore, the disk *i* has been applied by both contractive and torsional forces. The collective electromagnetic forces from all parallel disks make the CNT fiber contract and rotate.

The electromechanical rotation of CNT fibers provides promising applications in many fields. For instance, they can be used to fabricate high-efficiency rotational motors with a simple structure and high efficiency. **Figures 4**a and S4, Supporting Information, represent a typical experimental setup. A CNT fiber with a length of 4 cm was suspended above a glass substrate. A shaft such as another short CNT fiber with a length of 8.5 mm was attached onto its right side to hang an object, e.g., a piece of paper with a weight of 0.3 mg. Here the weight of the CNT fiber shaft was less than 1 μg and is negligible compared with the object. Therefore, the centroid of this subminiature pendulum can be designated as the center of the object. When a current was passed through the CNT fiber motor, the right part would rotate the shaft. A typical rotation of the shaft was recorded upon a pass with a pulsed current between 0 and 5 mA (Movie S6, Supporting Information). The perpendicular distances (*d*) between the paper center and glass substrate were determined using a frame-by-frame analysis, and the rotary angles were obtained from $\psi = \arcsin(d/r)$, where ψ and r were the rotary angle and the length of the pendulum, respectively. Here the highest rotary angle was determined to be ~9.5°, and the torque τ was calculated to be 4.2 nN m using $\tau = m \cdot g \cdot r \cdot \sin\psi$, where m and g were the mass of the pendulum (0.3 mg) and gravitational acceleration (9.8 m s^{-2}), respectively. The CNT fiber with length of 4 cm had a mass of ~4 μg, so this fiber motor could rotate and lift an object of up to 75 times its own weight and drive a pendulum with a radius of up to 1000 times its own in size.

The rotary angle ψ strongly depends on the passed current, and Figure 4b shows that the rotary angle gradually increases with an increase in current. The plot of $\sin\psi$ versus current is further used to investigate the relationship between torsional moment and current (Figure 4c). According to the fitting curve, $\sin\psi \propto I^2$, as $\tau = m \cdot g \cdot r \cdot \sin\psi$, so $\tau \propto I^2$. The stability of the fiber motor was further tested by using a pulsed current between 0 and 5 mA. As shown in Figure 4d, the rotary angles remain almost the same after 180 cycles. Furthermore, for the same pulsed current with frequency of 0.17 Hz, this fiber motor had been actuated for over 2400 cycles with a stable rotary angle.

In summary, as the lengthwise contraction and rotary torsion can occur in almost all available media, this spun CNT fiber may represent a general material for various fields including energy, biomedicine, sensing, and electronic engineering. In particular, the CNT fiber exhibits a light weight with a linear density of 100 μg m^{-1}, much lower than 10 mg m^{-1} for cotton and 20–100 mg m^{-1} for wool yarns, an excellent mechanical property with a specific strength 2.9 times that of T1000, the strongest commercial fiber, and a specific stiffness 3.9 times that of M70J, the stiffest commercial fiber, and exceptional electronic property with electrical conductivity up to 10^3 S cm^{-1}. In addition, tens to hundreds of CNT fibers have been easily twisted into macroscopic fibers which also exhibit the lengthwise contraction and rotary torsion, and the produced force could be further greatly improved, e.g., about twenty times that of individual CNT fibers if twenty five were twisted together. The combined remarkable properties may further provide CNT fibers with unique applications which remain challenging to conventional materials, e.g., aerospace devices.

Experimental Section

CNT fibers were spin-drawn from a CNT array grown on a silicon substrate by a chemical vapor deposition process.[9] The drawing rate was 2 mm s^{-1} with spinning rates from 1000 to 4000 rounds per minute for CNT fibers with both left- and right-handed rotations. In this work for

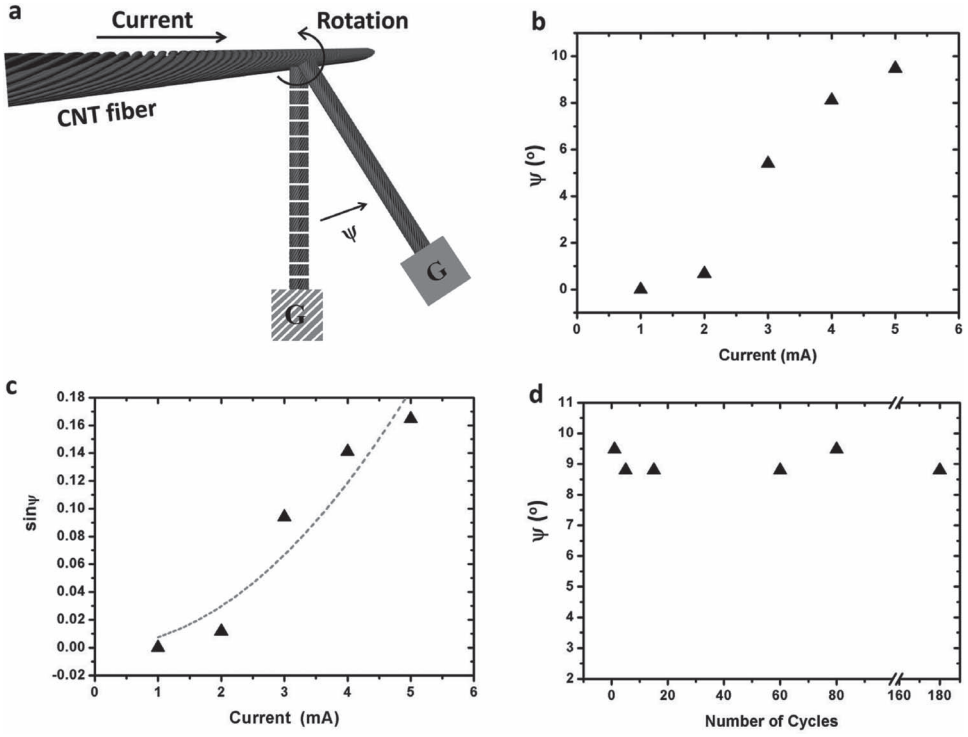

Figure 4. The use of a CNT fiber as an electric motor. a) Schematic illustration of the experimental setup. An object is attached to one end of a shaft with another end stabilized onto the CNT fiber. The object will be rotated from the left to the right upon the pass of the current. b) Dependence of the rotation angle (ψ) on the applied current. c) Dependence of the sine of rotation angle ($\sin\psi$) on the applied current. The dashed line is a fitting curve. d) Dependence of the rotation angle on cycle number upon the use of a pulsed current between 0 and 5 mA.

convenience, the CNT fibers were all obtained from the same array with a thickness of ~200 μm. The fabrication setup and the process are shown in Figure S1 and Movie 1 in the Supporting Information. Structures of CNT fibers were characterized by SEM (Hitachi FE-SEM S-4800). Optical microscopy (Olympus BX51) was used to monitor the torsional process of a CNT fiber. To trace the produced stress, a CNT fiber stabilized on the paper held with a gauge length of 5 mm was anchored onto a table-top testing instrument (HY0350 Table-top Universal Testing Instrument) with copper wires connected to a computerized Keithley Model 2400 Sourcemeter. The tested CNT fiber was tightly drawn from two ends prior to the passage of electrical current and recording of the stress.

For use in an electric motor, a left-handed CNT fiber with a length of 4 cm was first suspended with the ends stabilized on two glass slides. One end of a micrometer-sized shaft (e.g., another short CNT fiber) was then glued to the CNT fiber motor with another end being attached to the object, e.g., a small piece of paper with a weight of 0.3 mg. The lengthwise density of the CNT fiber was measured as ~1 μg cm^{-1} by thermogravimetric analysis (Shimadzu DTG-60H).

Supporting Information

Supporting Information is available from the Wiley Online Library or from the author.

Acknowledgements

This work was supported by NSFC (20904006, 91027025, 11004034), MOST (2011CB932503, 2011DFA51330), MOE (NCET-09-0318), STCSM (1052nm01600, 11520701400), SKPOC (2012CB921604), and General Motors Company. W. Guo and C. Liu contributed equally to this work.

Received: May 7, 2012
Published online: July 31, 2012

[1] M. Fennimore, T. D. Yuzvinsky, W. Han, M. S. Fuhrer, J. Cumings, A. Zettl, *Nature* **2003**, *424*, 408.
[2] Y. Yun, V. Shanov, Y. Tu, M. J. Schulz, S. Yarmolenko, S. Neralla, J. Sankar, S. Subramaniam, *Nano Lett.* **2006**, *6*, 689.
[3] T. Mirfakhrai, J. Oh, M. Kozlov, E. C. W. Fok, M. Zhang, S. Fang, R. H. Baughman, J. D. W. Madden, *Smart Mater. Struct.* **2007**, *16*, S243.
[4] A. E. Aliev, J. Oh, M. E. Kozlov, A. A. Kuznetsov, S. Fang, A. F. Fonseca, R. Ovalle, M. D. Lima, M. H. Haque, Y. N. Gartstein, M. Zhang, A. A. Zakhidov, R. H. Baughman, *Science* **2009**, *323*, 1575.
[5] J. Foroughi, G. M. Spinks, G. G. Wallace, J. Oh, M. E. Kozlov, S. Fang, T. Mirfakhrai, J. D. W. Madden, M. K. Shin, S. J. Kim, R. H. Baughman, *Science* **2011**, *334*, 494.
[6] a) . Q. Li, Y. Li, X. Zhang, S. B. Chikkannanavar, Y. Zhao, A. M. Dangelewicz, L. Zheng, S. K. Doorn, Q. Jia, D. E. Peterson, P. N. Arendt, Y. Zhu, *Adv. Mater.* **2007**, *19*, 3358; b) Z. Yang, T. Chen, R. He, G. Guan, H. Li, H. Peng, *Adv. Mater.* **2011**, *23*, 5636; c) S. Huang, L. Li, Z. Yang, L. Zhang, H. Saiyin, T. Chen, H. Peng, *Adv. Mater.* **2011**, *23*, 4707; d) L. Li, Z. Yang, H. Gao, H. Zhang, J. Ren, X. Sun, T. Chen, H. G. Kia, H. Peng, *Adv. Mater.* **2011**, *23*, 3730.
[7] M. H. Miao, *Carbon* **2011**, *49*, 3755.

[8] a) H. Peng, M. Jain, Q. Li, D. E. Peterson, Y. Zhu, Q. Jia, *J. Am. Chem. Soc.* **2008**, *130*, 1130; b) T. Chen, Z. Cai, Z. Yang, L. Li, X. Sun, T. Huang, A. Yu, H. G. Kia, H. Peng, *Adv. Mater.* **2011**, *23*, 4620.
[9] K. Koziol, J. Vilatela, A. Moisala, M. Motta, P. Cunniff, M. Sennett, A. Windle, *Science* **2007**, *318*, 1892.
[10] H. Peng, X. Sun, F. Cai, X. Chen, Y. Zhu, G. Liao, D. Chen, Q. Li, Y. Lu, Y. Zhu, Q. Jia, *Nat. Nanotechnol.* **2009**, *4*, 738.
[11] a) T. Chen, S. Wang, Z. Yang, Q. Feng, X. Sun, L. Li, Z. Wang, H. Peng, *Angew. Chem. Int. Ed.* **2011**, *50*, **1815**; b) T. Chen, L. Qiu, Z. Yang, H. G. Kia, H. Peng, *Adv. Mater.* **2012**, *24*, DOI: 10.1002/adma.201201893.
[12] P. M. Chaplya, M. Mitrovic, G. P. Carman, F. K. Straub, *J. Appl. Phys.* **2006**, *100*, 124111.
[13] A. Hall, M. Allahverdi, E. K. Akdogan, A. Safari, *J. Electroceram.* **2005**, *15*, 143.
[14] M. Shahinpoor, K. J. Kim, *Appl. Phys. Lett.* **2002**, *80*, 3445.
[15] E. Smela, *Adv. Mater.* **2003**, *15*, 481.
[16] D. B. Li, R. Baughman, T. J. Huang, J. F. Stoddart, P. S. Weiss, *MRS Bull.* **2009**, *34*, 671.
[17] J. Madden, N. A. Vandesteeg, P. A. Anquetil, P. Madden, A. Takshi, R. Z. Pytel, S. R. Lafontaine, P. A. Wieringa, I. W. Hunter, *IEEE J. Oceanic. Eng.* **2004**, *29*, 706.